

Chapter 7

Mastering Nano-objects with Photoswitchable Molecules for Nanotechnology Applications

R. Barillé, E. Ortyl, S. Zielinska and J.M. Nunzi

Abstract Advance in the fabrication of nano-objects becomes more important for the development of new nanodevices with local properties leading to new functional devices. In this direction, the assembly of nanometer-scaled building objects into device configurations and functionalization is a promising investigated research field in nanotechnology. Optical recording and photofabrication techniques that exploit changes in material properties have gained importance, and there is a requirement for a decrease of the dimensions of the recording and processing surfaces. Photochromic materials leading to submicron structures responding to stimuli and in particular light are the best materials that exhibit multifunctional behaviors. Photomechanical properties of azopolymers show the perfect performance in photoinduced nanopatterning and reshaping by tailored light fields. Azopolymer nanostructures are then recognized as an excellent choice for a broad range of fundamental and applied research in modern nanotechnology. This chapter shows how polymer nanofilms, nanotubes, nanospheres, or nanowires containing azobenzene can be controlled by light for new photonics applications. Spatially confined excitation of unidirectional motions could make possible the local control of mechanical properties of the material and its structuration. The unprecedented flexibility of the reported photofluidization lithography with this material allows producing well-defined structures as lines, ellipsoids, rectangles, and circles at azopolymer surface with several tenth nanometers structural features.

R. Barillé (✉)

Moltech Anjou, CNRS UMR 6200, PRES UNAM, University of Angers, 2, bd Lavoisier, 49045 Angers, France
e-mail: regis.barille@univ-angers.fr

E. Ortyl · S. Zielinska

Department of Polymer Engineering and Technology, Wrocław University of Technology, 50-370 Wrocław, Poland

J.M. Nunzi

Department of Chemistry, Queen's University, 90 Bader Lane, K7L 3N6 Kingston ON, Canada

7.1 Introduction

A first look on the scientific material journals reveals that the past decade has indeed seen transformative challenges in the scientific landscape due to nanoscience and nanotechnology advances. Optical recording and photofabrication techniques that exploit changes in material properties have gained importance, and there is a requirement for a decrease of the dimensions of the recording and processing surfaces. Advance in the fabrication of nano-objects becomes more important for the development of new nanodevices with local properties leading to new functional devices [1]. Many directions can be taken for their realizations. One is the reduction of the way information can be stored and how tightly irradiating light or stimuli can be focused. The other direction exploits the fabrication of nano-objects reaching the nanometer-scale dimensions for configuring these nano-objects in order to contain information. The techniques used to generate nanoscale structures can commonly be categorized as top-down and bottom-up approaches.

For this reason, photochromic materials have attracted the focus of researchers as promising media for different applications as data recording, storage, and readout in both nonlinear optics and holography [2]. Among these materials, aromatic azo compound holds a prominent place. Photochromic transformations in azo compounds are related to the photoinduced *trans*–*cis* isomerization of their molecules. Photoinduced isomerism of azobenzene proceeds with large structural change as reflected in the dipole moment and change in geometry. During their photoinduced excitation, *trans* monomers are transformed into the *cis* form. The isomerization process can have a deep effect on the physical and optical properties of materials which contain the azobenzene chromophore as a parent molecule or as a dopant. Azo labels can be selectively attached to the side chains, main chains, cross-links, or chain ends of the polymer. One of the most interesting phenomena associated with the photoisomerization process is massive macroscopic motions of the polymer chains leading to physical deformation of the material well below the glass transition temperature. With this molecule, polymer materials are changed from structural materials to functional materials and the current trend is to employ the azobenzene moiety as a trigger to induce morphological changes which can be light driven [3, 4].

Azopolymer nanostructures are recognized as an excellent choice for a broad range of fundamental and applied research in modern nanotechnology. Owing to unique photomechanical properties of azopolymers, these nanostructures show the perfect performance in photoinduced nanopatterning and reshaping by light fields. Unprecedented flexibility of recently reported photo-fluidization lithography allows producing well-defined lines, ellipsoids, rectangles, and circles at azopolymer surface with several tenth nanometer structural features [5].

We present in this review how the structure properties of polymer nanofilms, nanotubes, nanospheres, or nanowires containing azobenzene can be controlled

by light for new photonics applications. Spatially confined excitation of unidirectional motions could make possible the local control of mechanical properties of the material and its structuration.

In this goal, the production of uniform-sized nano-objects is important. We show the possibilities given by these nanosize objects in view of future applications in photonics and biology. We will split the different parts of the chapter as a function of the topology of the material. The first part will deal with 2D materials (nanofilms). The second part will be devoted to nanotubes corresponding to 1D materials. Finally, if we reduce by an order the topology dimension of the nano-objects, we end up to 0D materials with nanospheres. In the different parts, we will give technological applications of these nano-objects.

7.2 Nanofilms

Polymeric ultra-thin films or nanofilms show noteworthy properties making them potentially useful for several applications in photonics and metrology [6, 7]. They are usually characterized by a thickness lower than one micron meter. Azopolymer nanofilms are good candidates for top or bottom techniques used to generate nanoscale structures. Irradiation of a flat isotropic azopolymer film surface with an intensity distribution of a plane polarized light results in a transfer of an optical pattern to the film surface known as a surface relief grating (SRG). The pitch of the pattern can be controlled by the angle producing the interferences. Typically, two interfering beams are used to create a pattern. The obtained photoinduced surface patterns can be used either directly as functional optical elements or indirectly to microstructures or nanostructures as other optical materials. Once the azopolymer films have been patterned, they can be used as templates to create patterns in other materials [8]. However, the bottom-up approach has the advantage of cheaper setup, operating costs, and the ease of use, but cannot offer the accuracy in producing the shape and location of nanostructures that demonstrate the top-down techniques. Different alternatives to the conventional method with interference pattern are presented using a single laser beam only or with an additional white light. The process uses the molecular self-organization of the photoinduced material.

7.2.1 SRG with a Single Beam

The use of a single beam to induce a pattern on the surface is a challenge because it requires anticipating molecular reactions and controlling the nanoscale pattern. Most of the experiments with one single beam are done with a light illuminating a mask [9]. A photolithographic technique involving the exposure of azopolymer as a photosensitive material through soft conformable phase mask was done [10]. The conformable phase mask was made of transparent flexible materials such as

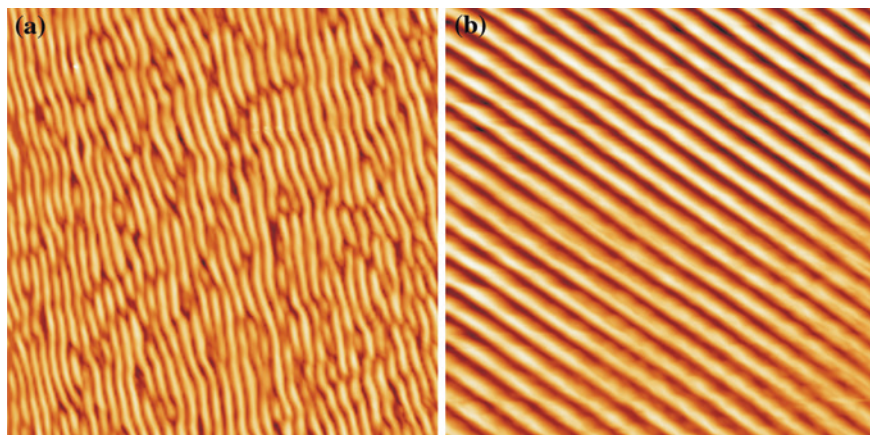
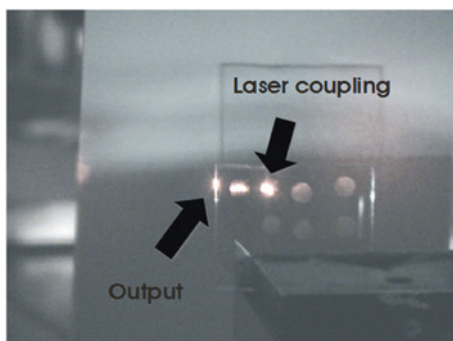


Fig. 7.1 Comparison of surface relief gratings produced by illuminating an azopolymer thin film with **a** one beam by molecular self-organization and **b** by two beam interference

Fig. 7.2 Light coupling of a laser beam in a polymer thin film with a SRG



polydimethylsiloxane (PDMS). Passage of light through the phase mask generates a complex 3D intensity distribution of light in the azopolymer material and nanoscale patterns. Very recently, a multistate storage of a single beam polarization was achieved and read out in a polymer material. This original technique uses only one beam with a controlled polarization to photoinduce a SRG whose wave vector direction depends on the light polarization [11]. Different polarizations of the input laser beam, for example 0° , 30° , 60° , and 90° , can be stored on the surface of azopolymers. Figure 7.1 compares the topography of the surface for the two techniques. In both techniques, the amplitude of the grating is similar with a depth of 50 ± 5 nm. The surface pattern obtained with a single beam is slightly irregular but allows its use in different applications. Figure 7.2 gives one example showing the coupling of light in the thin film with a grating obtained by surface molecular self-organization.

7.2.2 SRG with Incoherent Light

In the goal to find low cost methods to photoinduce SRGs on the surface of thin films, no real solutions were proposed because the general opinion about SRGs is that patterning of photoactive systems needs coherent light.

In the standard setup of SRG inscription on azo dye-based photoactive polymers, the photoactive molecules are excited by an illumination pattern. It was recently showed that a well-defined SRG can be induced in an azopolymer film by the combination of a low-power coherent laser beam with another high-power incoherent and unpolarized beam [12]. It appears that the low-power beam carries information about pitch and orientation of the diffraction grating that is transferred to the surface illuminated by the incoherent light (Fig. 7.3). In this way, a simple system allowing figuring out the minimal requirements to organize disordered materials by an incoherent light into well-organized structures was found. This result showed experimentally that random motions plus information exchanges lead to molecular self-organization. Information is then exchanged locally by the nanorelief of the polymer surface.

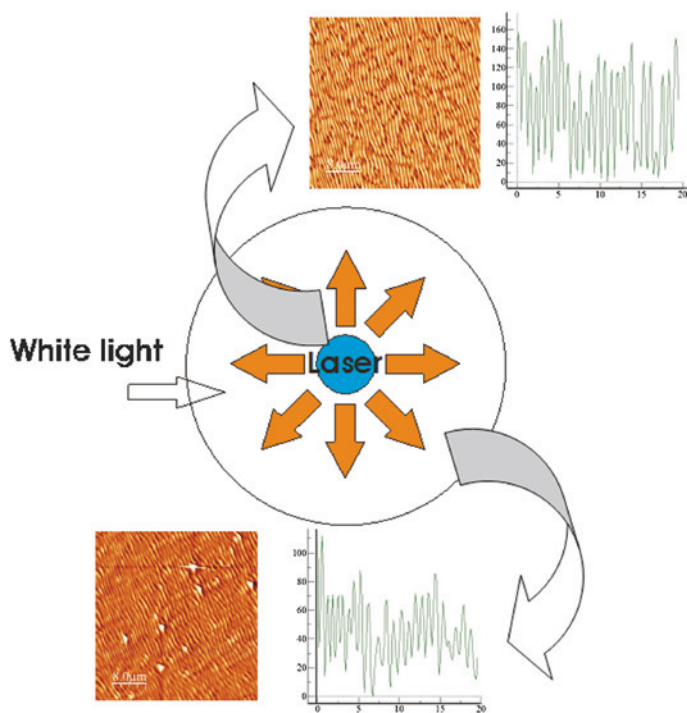


Fig. 7.3 SRG produced on the whole surface illuminated by the superposition of a low-power laser beam with a high-power incoherent light

7.2.3 Applications

SRG can find large applications in photonics as waveguide coupling [13] or sensor [14]. The fabrication of a hologram with a single beam can be advantageous in the special case of optical metrology and atmospheric turbulence. Outdoor environment has a significant impact on the quality of a laser beam propagating through the atmosphere over long distances. A method was proposed to measure the effect of turbulence influencing a laser beam with basically this idea: The spatial deformation of a laser propagating in atmospheric turbulence cannot be suppressed but can be used to discriminate the laser parameters influenced by the turbulence. A photochromic material able to self-organize the molecular thin-film surface in relief gratings was used. The contribution of the turbulence when a laser beam passes through a turbid medium with a non-uniform refractive index was measured [15]. The modification of the laser beam parameters modifies the regular written structuration of the thin film. This modification was analyzed by observing the diffraction pattern obtained when the laser beam is diffracted on the surface pattern. This new measurement was simple, was easily implemented, and gave absolute values of atmospheric turbulence (C_n^2) with a previous calibration [16].

In biology, a simple and easy technique to produce erasable and directly in vitro submicron-scale SRGs for the guidance of neurons with a new biocompatible photoswitching material and a single-step laser irradiation was demonstrated [17]. The material uses a photoresponsive polymer with azo chromophores. The glass surface for deposition of chromophoric polymers was modified to be able to form diffraction gratings and resistant to defoliation in aqueous solutions. Methacrylate terpolymers containing 2-hydroxyethyl group in side polymer chain was used to change the glass surface [18]. The results showed that cells sense ultrafine substrate topographies. Nanogrooves acted as scaffolds providing directional cues that guided PC12 cell alignment and orientation similar to microscale grooves.

7.3 Nanotubes

Nanotubes or tubular nanostructures have attracted a great deal of interest during the past decade because of their potential applications in ultrafiltration, catalysis, medicine, or sensors [19]. Tubular nanostructures can be prepared by various synthesis methods. The template synthesis method is regarded as a simple and very effective way for preparing various materials, including polymers, and metals [20]. Porous alumina template synthesis is one of the most commonly used methods because of the walls exhibiting a high surface energy. Researchers have used various kinds of membranes such as polycarbonates and anodized alumina membranes as templates for the fabrication of nanotubes and nanorods. The polymer nanotubes can be obtained by wetting the porous templates with polymer melts

or solutions. Such novel nanostructures are expected to provide new functions in optoelectronic and biological applications that cannot be attained with conventional spherical nanoparticles. The synthesis of azopolymer can lead to promising applications due to the surface or geometric modifications by molecular mass transport.

7.3.1 Fabrications

Nanostructures with extraordinarily small diameters were prepared with the method of wetting of porous anodic alumina membrane templates whose porosity consisted of an array of parallel and straight channels, as such low diameters are impossible to be obtained using lithographic methods. This template method has previously been shown to be capable of efficiently forming nanotubes for a variety of organic materials [21].

The alumina membrane filters (Anodisc) had a diameter of 13 mm and thickness of 60 μm . The cylindrical pores had uniform diameters, and each of these pores is viewed as a baker, in which an object of the desired material is shaped. The pores in the membrane had monodispersed diameters of 100 nm. An azopolymer nanocylinder was obtained in each pore. Figure 7.4a shows a scanning electronic microscope image of dispersed nanotubes. The average monodispersed diameter of the nanotubes was found to be 100 nm.

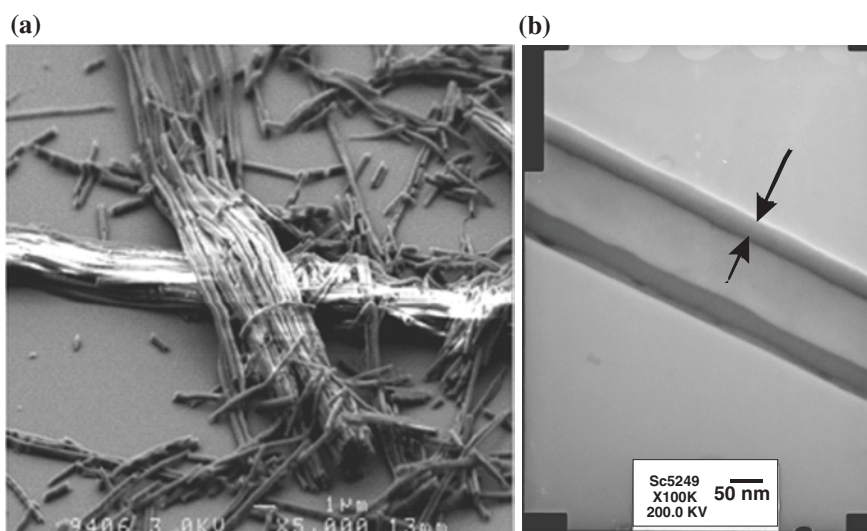


Fig. 7.4 **a** SEM of azopolymer nanotubes prepared with a 200 nm pore diameter Anodisc membrane, **b** TEM image of one nanotube. The nanotube wall thickness indicated by *arrows* is about 15 nm

The length depends on the different chosen areas on the sample but an average length of 10–15 μm was measured. Figure 7.4b shows cross sections of nanotubes dispersed on a grid and observed with TEM. A typical inner wall of 15 nm is measured. The TEM observations confirm the hollow core structure of the nanotubes with a constant cross section along axis.

7.3.2 *Nanostructuring of Nanotubes*

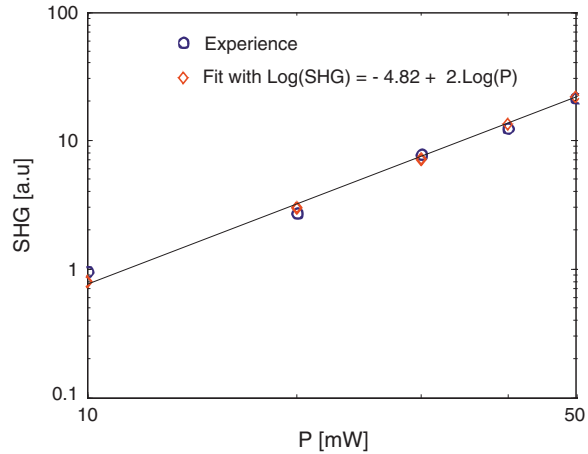
Periodic structures in the submicrometer scale are in high demand for many applications ranging from electronics to photonics, and large results have been obtained but less on nano-objects [22]. Up to now, patterning of structures was possible on the surface of thin films. We recently demonstrate the possibility to inscribe a nanostructure on the surface of azopolymer nanotube with laser illumination [23, 24]. In this view, assembly of nanometer-scale building blocks into device configurations with different individual patterns could be promising for tag of information and data storage. Building patterns on the surface of nanometer objects permits optical processing for nanoscale engineering and for biotechnologies. At this scale, only instruments with enough resolution as near-field optical microscope are able to fit the pattern dimension required.

7.3.3 *Nonlinear Effects with Nanotubes*

Beyond all nonlinear phenomena, the second harmonic generation (SHG) is particularly interesting because it can be generated through surface interactions, local imperfections, and deformations resulting from the assembly of the nano-objects on the surface. The use of polymer nanotubes dispersed on the surface as randomly oriented mess can give rise to interesting nonlinear phenomena which are influenced by the structure of the nano-objects.

For the needs of the SHG investigation, the sample has been placed on X, Y, Z, θ stage and in the focal point of a x50 objective microscope (Olympus SLMPLN50X, numerical aperture = 0.45) with a diffraction-limited spot diameter of about 1.8 μm . The angle θ , defined between the normal to the surface of the sample and the optical axis, is chosen to maximize the SHG signal. The X, Y, Z motorized displacement stages were controlled in order to keep the focal point in the plane of the sample. The exciting beam was provided by a Tsunami Ti/sapphire tuneable laser (670–1,100 nm) with 120-fs pulse duration and 80 MHz repetition rate. The polarization and the power of the incident beam on the sample have been adjusted with a half-wave plate and a Glan-Taylor polarizer. The light exiting the sample has been collected by a second microscope objective and then directed to the input slit of a spectrometer. The spectrum was then recorded by a fast liquid nitrogen-cooled CCD camera (Princeton research) at the exit plane of the monochromator. A Schott BG 39 filter eliminated the fundamental laser wavelength.

Fig. 7.5 Log-log plot of the SHG intensity of dispersed nanotube on glass substrate versus pumping intensity ($\lambda = 750$ nm)



At a wavelength of 750 nm, employing a 10 mW laser power (corresponding to 125 pJ per pulse and 400 W peak power), nearly uniform SHG signal over the surface of the sample has been obtained.

To ensure that the acquired signals were entirely related to second-order nonlinear processes, several precautions were taken. Firstly, the dependence of the SHG response upon the incident laser power has been checked by performing SHG measurements, with few nanotubes dispersed on the glass substrate. An area has been chosen, where nanotubes with equal length were well dispersed, and less than 10 nanotubes were within the laser-beam-spot-irradiated area. The average power of the laser has been varied, without changing any other experimental parameters, while recording the SHG signal coming from the same area on the sample surface. An upper threshold of 50 mW has been used to avoid damaging of the sample. In Fig. 7.5, the SHG efficiency as a function of the incident laser power is plotted in logarithmic scales. As it can be seen in the same figure, the slope of the fitted line is equal to 2 confirming the quadratic dependence of the signal with the input power, verifying the second-order nonlinear origin of the signal and that no saturation of the response was taking place. Similar results have been obtained in other areas on the sample, while the contribution of the glass has been found to be negligible under the same experimental conditions and even higher laser powers.

Based on these SHG findings, further measurements have been carried out in order to investigate the possibility to detect signal coming from only one nanotube. During this investigation, the power of the fundamental beam was fixed to 10 mW with vertical (s) polarization. In Fig. 7.6, typical SHG spectrum (blue line) of a nanotube is obtained using 3-min integration time. We use a spline fitting curve (red line) for a better estimation of the intensity peak of the spectrum. The signal to noise ratio is 2.5. Long exposure time has been chosen in order to increase the signal to noise ratio without increasing the laser power, which could possibly result in

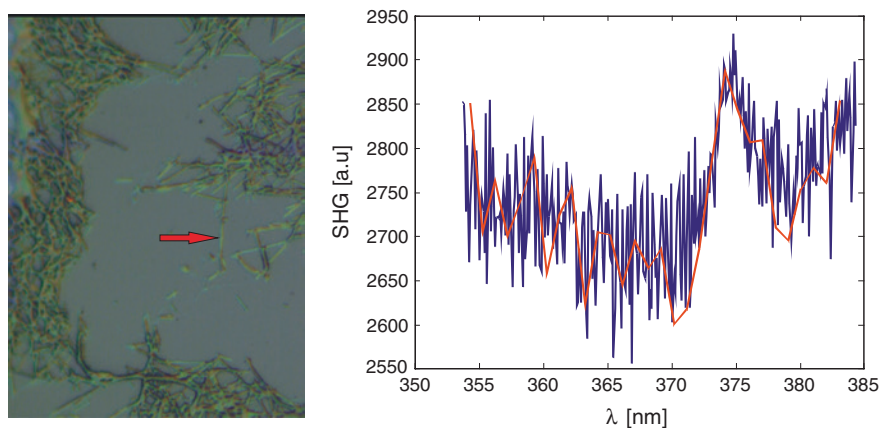


Fig. 7.6 High magnification optical image of azopolymer nanotubes dispersed on a glass substrate (*left*) with the SHG intensity measured on a single nanotube (*right*). The *arrow* indicates where the SHG measurement has been done

the damage of the sample. This long exposure time could be reduced by choosing a laser with a laser fundamental wavelength out of the range of our current laser wavelengths in order to limit the SHG absorption by the sample in the light path.

The investigated area, which includes only one nanotube, is shown in the upper part of the same figure and has been checked after the measurements to verify that no damage of the sample during the irradiation has been done. The peak at a wavelength of 375 nm confirms the existing second harmonic signal generated from one nanotube. This result of high SHG intensity with a nanotube correlates collagen fiber SHG results [25]. Moreover, the SHG efficiency has been mapped over an area on the film providing 2D SHG mapping of the sample surface (Fig. 7.7). The area has a size of 100 μm by 80 μm and has been scanned with two different polarizations of the laser beam (s and p). It is interesting to note the big contrast between the two polarizations. For a vertical (s) polarization, an intense SHG has been observed, while in the case of horizontal (p) polarization, almost no signal has been obtained, under the same experimental conditions.

All the nanotubes were randomly laid down on the surface scanned by the laser, so the negligible signal in the case of horizontal polarization cannot be attributed to the geometric configuration of the nanotubes. We make the assumption that the axially transverse alignment of the molecules during the fabrication of the nanotubes gives this anisotropy concerning the SHG efficiency.

A polar diagram in Fig. 7.8 gives the integrated SHG intensity of the whole sample containing nanotubes dispersed on the surface as a function of the linear laser beam polarization. During this measurement, the laser beam has been focused by means of a microscope objective with a low magnification ($\times 10$, $\text{NA} = 0.25$) and the signal was collected with a photomultiplier. The maximum response of the sample is obtained for a laser beam polarization of 90° , in agreement with our previous findings.

Fig. 7.7 SHG mapping of the surface of dispersed azopolymer nanotubes for the vertical polarization (*above*) and the horizontal polarization (*below*) of the laser beam. In both images, the laser beam intensity is the same

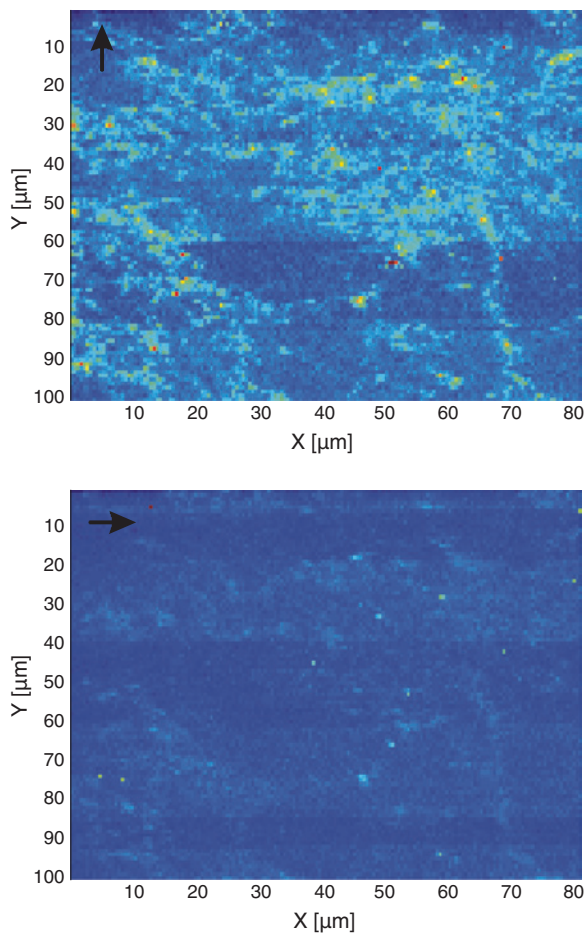
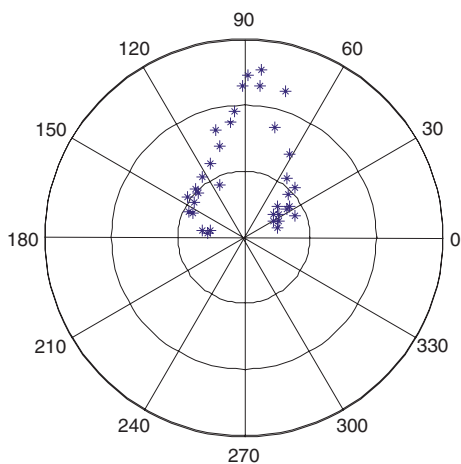


Fig. 7.8 Polar diagram for SHG measurements of the dispersed azopolymer nanotubes on the surface of a glass substrate



In order to shed light into the fact that different laser polarizations result in different SHG intensities, complementary measurements with a confocal Raman microscope have been carried out. These studies were expected to reveal information related to the conformation and molecular order of the azopolymer nano-objects. We show that there is a strong dependency between the intensity of certain Raman bands and the orientation of the nanotube with respect to the incident laser light.

Raman spectra were taken with a confocal Raman microscope (Renishaw in-Via) with a laser wavelength at $\lambda = 647$ nm and 600 lines/mm grating. The laser wavelength is chosen far from the absorption band of the material. The CW laser power was set to 1.0 mW to avoid denaturation of the sample. The laser has a polarization ratio of 100:1. The laser beam polarization direction is referred as perpendicular or parallel to the substrate. However, the measurements can be considered as unpolarized because no analyzer was used. The integration time is fixed to 10 s. The microscope objective used for focusing the incident laser beam and collecting the Raman signal has a high magnification ($\times 100$, NA = 0.75). We have checked that the sample's substrate did not contribute to the measured Raman signal.

The anisotropy of Raman bands has its origin in the preferential orientation of vibrating molecular fragments with respect to the nano-object axis and incident polarization orientation [26]. We consider how alignment of nanotubes along the two axes x and y will influence the observed anisotropy and how we can use Raman anisotropy measurements to probe the molecular alignment. To account on this possibility, we choose two individual isolated nanotubes on the sample in the vertical and horizontal position with two different linear laser beam polarizations as it is described in Fig. 7.6. The Raman spectra shown were obtained on nanotubes with long axes aligned in parallel and perpendicular with respect to the polarization of the incident laser beam in Fig. 7.9.

Fig. 7.9 Scheme of the confocal Raman measurements on a single nanotube. The chemical structure of the azopolymer sample is inserted in the figure

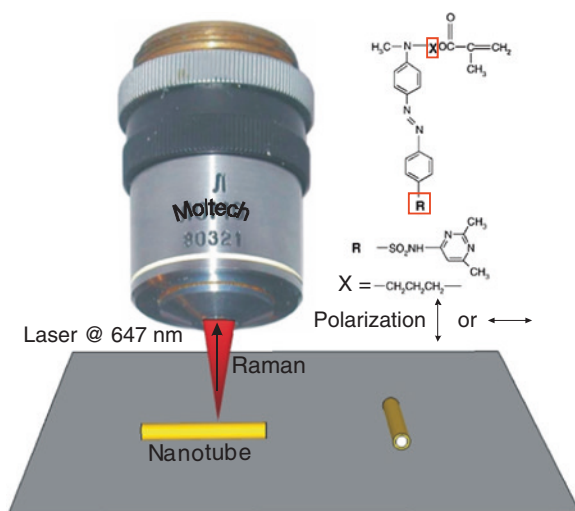
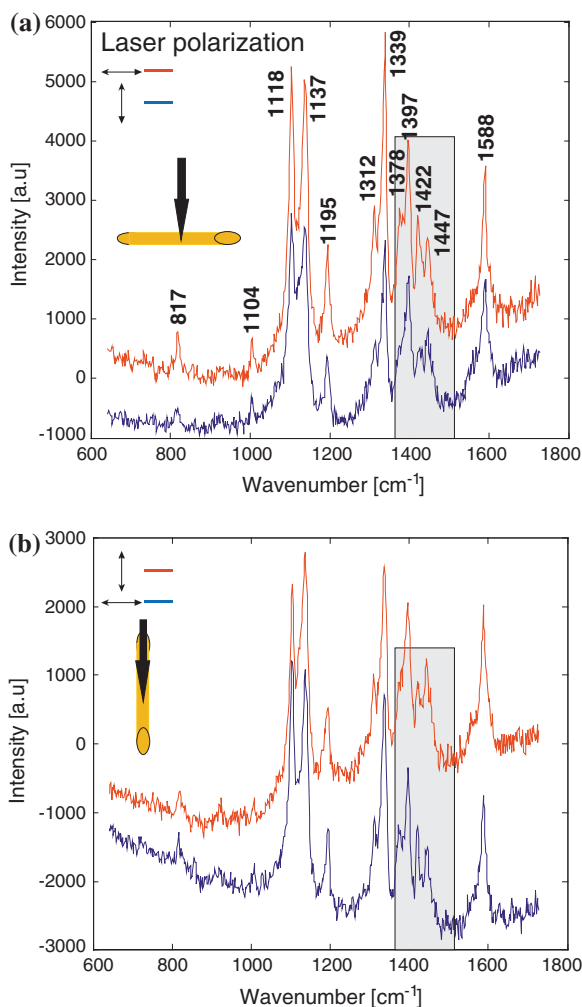


Fig. 7.10 Raman spectra obtained with the confocal Raman microscope and taken on a single azopolymer nanotube for two incident laser beam polarizations. The orientation of the nanotube is inserted. The *gray squares* indicate the selected bands that show the strongest anisotropic Raman scattering



The experimental Raman spectra have first been processed to eliminate the signal background offset with a first-order polynomial. The final flattened Raman spectra are shown in Fig. 7.10. They display a difference in intensity offset between the vertical and horizontal polarization which does not affect the analysis based on the spectrum's peaks. The spectra present eight main bands representing the different vibrations of the molecule shown in the inset of Fig. 7.10. They feature the characteristic of azopolymer bands.

Very fine details of the spectrum in the window from 1,000 to 1,600 cm^{-1} are present with double peaks not measured in previous studies on azobenzene materials [27]. The band assignments for the Raman spectra of nanotubes were made by referring to Raman spectra of various azobenzene derivatives for which

vibrational assignments have been well established [28]. We have four double peaks with intense signals at $1,104\text{ cm}^{-1}$ ($\nu(\Phi\text{-N})$, 18a), $1,137$ and $1,195\text{ cm}^{-1}$ ($\delta(\text{CH})$ ring 9a and 9b), $1,339\text{ cm}^{-1}$ ($\nu(\text{NO}_2)$), $1,397\text{ cm}^{-1}$ ($\nu(\text{N}=\text{N})$), $1,422$ and $1,447\text{ cm}^{-1}$ ($\delta(\text{CH})$ ring 19a and 19b). The assignment of the main bands of azobenzene at $1,137\text{ cm}^{-1}$, $1,447\text{ cm}^{-1}$, and $1,588\text{ cm}^{-1}$ as the C–N, N=N, and phenyl C=C stretches, respectively, is consistent with the available literature [14]. The Raman frequencies in the spectrum present a cluster of three bands of almost equal intensities at $1,312\text{--}1,339\text{ cm}^{-1}$, $1,378\text{--}1,397\text{ cm}^{-1}$, and $1,422\text{--}1,447\text{ cm}^{-1}$. These bands in the spectra feature the characteristic of the *trans*–*cis* isomerization and are assigned to the –N=N– stretching mode with a contribution from the phenyl ring mode (ν_{19}). The frequency of the –N=N– stretching band of azobenzene derivatives is very sensitive to the conformation around the –N=N– group. Moreover, the $\nu(\text{NO}_2)$ mode at $1,339\text{ cm}^{-1}$ is oriented along the long molecular axis of the *trans*-shape azobenzene chromophore and is a good probe to estimate the orientation of the rod-shape azobenzene chromophore. We focus our analysis on the peak at $1,339\text{ cm}^{-1}$, and the peaks in the frequency range from $1,330$ to $1,430\text{ cm}^{-1}$ corresponding to the gray square in Fig. 7.10.

The peak at $1,339\text{ cm}^{-1}$ and its intensity ratio compared to the peak at $1,312\text{ cm}^{-1}$ do not show a significative variation when the polarization is changed. This mode is sensitive to reorientation mechanisms in the light-induced isomerization meaning that no molecular movement took place in the nanotube. No laser light with a wavelength matching the absorption spectrum of the azopolymer nanotubes has been sent to the sample. Then, no photoinduced translation diffusion motion of the azo dyes during isomerization has been involved before our measurements.

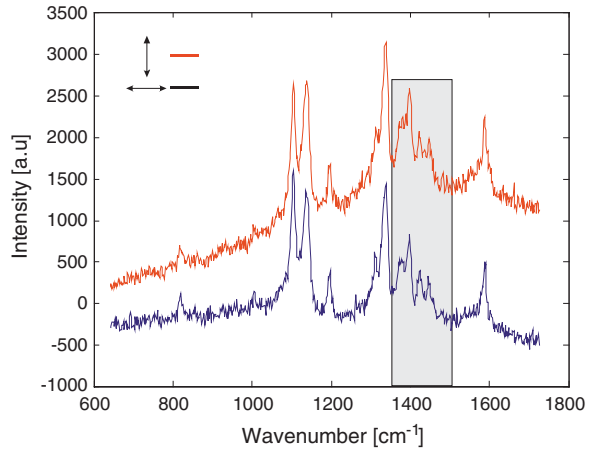
Two double peaks are present: one for $\nu_1 = 1,378\text{ cm}^{-1}$ and $\nu_2 = 1,397\text{ cm}^{-1}$ and the second one for the frequencies $\nu_3 = 1,422\text{ cm}^{-1}$ and $\nu_4 = 1,447\text{ cm}^{-1}$. The first peak at $\nu_1 = 1,378\text{ cm}^{-1}$ exhibits an orientation-dependent intensity. This intensity vanishes when rotating the polarization by 90° , whereas the peak at $1,378\text{ cm}^{-1}$ stays with nearly the same intensity.

Such behavior is also observed for the band at $1,422$ and $1,447\text{ cm}^{-1}$. We find again this variation of intensity when the nanotube is rotated by 90° . Raman spectra with the nanotube long axis aligned in the vertical direction confirm the polarization orientation-dependent intensity.

It is clear that the bands at $1,378$ and $1,422\text{ cm}^{-1}$ are less intense when the polarization is perpendicular or when the nanotube is oriented in the vertical direction. They show an enhanced Raman intensity in the parallel direction of the polarization. The variation of the Raman bands shows that all the molecular bonds at $1,312$, $1,378$, and $1,422\text{ cm}^{-1}$ are oriented parallel to the nanotube axis. The $1,339\text{ cm}^{-1}$ of the phenyl ring mode possesses a similar orientation. The anisotropic scattering for these bands indicates that the most probable orientation of the molecules is in the direction of the nanotube long axis [29]. The intensity of the spectra is sensitive to the average molecular orientation of the molecules and gives a maximum for one polarization.

Raman scattering measurements on the whole surface of the nanotubes are presented in Fig. 7.11. They do not present polarization orientation-dependent intensities as we have found in the case of the Raman measurements on individual nanotubes.

Fig. 7.11 Raman spectra obtained with the confocal Raman microscope with a low magnification of the microscope objective on large number of randomly dispersed nanotubes



We attribute this result to the fact that the signal emanates from a mixing of randomly oriented nanotubes. The small difference in the peak intensities is then difficult to be observed with the intensity resolution of the utilized instrument. Previous experiments on collagen allowed the observation of different spectra with far-field Raman measurements, when the sample is aligned in parallel or perpendicular with respect to the polarization of the incident laser [30] but the sample presented highly collagen structures with well-defined uniaxial parallel-aligned collagen fibrils contrary to our ample where the nanotubes are dispersed on the surface.

Confocal Raman measurements and polarized scanning near-field experiments on structured thin film electrically poled with a wire poling scheme have revealed a strong polar ordering of the azobenzene chromophores [31]. Moreover, concerning the SHG study, s polarization SHG measurements in this study resulted in a higher SHG response compared with those carried out with the p-polarized laser beam. After calculations, the authors showed that molecular orientational distribution calculations had a polar asymmetry along the reference direction normal to the film plane. Raman and SHG are two complementary measurements where the optical contrast relative to polar orientations is exclusively observed in SHG [32]. Nanotubes are hollow cylinders with extreme thin wall thickness. The high confinement of material in surface during the template fabrication leads to a molecular radial self-assembly and organized along the nanotube long axis. Then, inside the nanotubes with no light previously sent to photoisomerize the molecules and no electric field applied, azo molecules present a natural polar distribution along the Z reference revealing a quite efficient poling in the nanotube. Assuming the molecular backbone lies perpendicular to the circular geometry of the nanotube, considering molecular vibrations with a highly uniaxial Raman tensor and the principal axis is coincident with the polymer chain axis, the mechanism of SHG in the case of p-polarized laser beam, whatever the random distribution of the nanotubes on the glass surface, can be then well explained. However, a small

component of the angular orientation of the molecules in the horizontal direction explains the nonzero variation of the polarizability and the polarization orientation-dependent Raman spectra, if the electric field is applied parallel or perpendicular to the molecular axis. Precise angular distribution of molecules inside the nanotubes requires further, complete calculations, which are not necessary in the context of further developments of azopolymer nanotubes for photonic or biological applications.

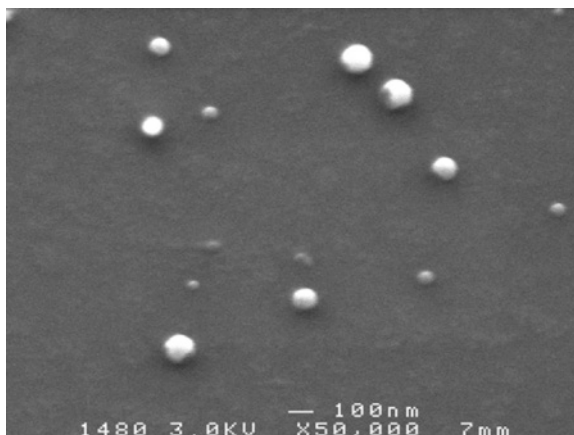
7.4 Nanospheres

Current interest in the properties of polymers (mechanical, electrical, ...) confined into nanometer scale is very intense, both from the fundamental and practical perspectives. Polymers are widely used in nanofabrication processes such as wires of nanometer-scale diameters, nano-imprinting, and nanoscale polymeric particles. Confined polymers are central to a broad range of advanced materials and emerging nanotechnologies, with applications including biomaterials, micro- and optoelectronics, and energy capture/storage, among others [33]. Nanometer-sized functional particles are attractive for optical, electrical, magnetic, and biological applications. Besides cutting-edge fabrication strategies, control over the changes in properties induced by nanoscale confinement is a central issue to be taken into account. Moreover, in addition to size, the shape of a nanoparticle was reported to be crucial, for example, how it interacts with light.

For several years, modification of the physical properties due to size effects when approaching nanometer lengths in glass forming systems in general, and in polymers in particular, has been strongly debated. Among the different properties, variations of the glass transition of confined polymers as in thin nanometer-thickness films have motivated a good number of experimental works [34]. Confinement experiments in polymer systems in general have been considered as a very elegant way of probing the existence of a correlation length (ξ) of cooperative motions that produces molecules under light [35]. For azobenzene molecules, the thermal relaxation from the *cis* state to the *trans* state completes an optomechanical cycle that could leave the azobenzene group in a new orientation leading a mass transport and a surface modification when the molecule is grafted to the polymer chain of the polymer matrix. It is potentially interesting to study the molecular mass transport in geometric system with a restricted freedom of movements.

Although there are tremendous potential advantages of using anisotropic nanoparticles like nanorice instead of conventional spherical nanoparticles, the development of controlling such shape on the nanoscale is in its early stages. Even though polymer nanospheres have commonly been produced, the terminal shape modification of a large number of polymer nanoparticles or individual ones into nanorice or nanospears has remained a challenging task. If functional polymer nanoparticles can be shaped in the desired forms on the nanoscale, they can easily be functionalized to have much enhanced multifunctional properties using them as nanotemplates or substrates.

Fig. 7.12 SEM image of azopolymer nanospheres



7.4.1 Fabrication of Azopolymer Nanospheres

The azopolymer was dissolved at 50 mg/ml in tetrahydrofuran (THF). The nanospheres were prepared following the method used for aggregate formation from polystyrene-poly (acrylic acid) block copolymers micelles [36]. Deionized water was added dropwise into the THF solution. When micellization occurs, the nanospheres are dropped on a glass substrate. Density of the nanospheres on the surface is about $9 \mu\text{m}^{-2}$. Figure 7.12 presents a scanning electron microscope (SEM) image of the nanospheres dispersed on the surface of a microscope glass slide. We can estimate their external diameter by statistical analysis of the image around $84 \pm 10 \text{ nm}$.

7.4.2 Photomechanical Effect on Azopolymer Nanospheres

The shape modification of azopolymer nanoparticles used a white light with enough power to avoid melting of the nanospheres onto the sample. Figure 7.13 shows an AFM image of two nanospheres before and after irradiation of the sample surface with the incoherent white light. After irradiation, the nanosphere width has expanded. A cross section in the horizontal and vertical directions of nanosphere surface topographic profiles before and after irradiation have shown that the sphere has been expanded almost uniformly in the film plane, with a recorded increase of 20 % for the horizontal cross section and 35 % for the vertical cross section in the substrate plane. The photoelastic force exerted by light was estimated around $1 \mu\text{N}$ corresponding to an order of magnitude larger than typical forces needed for the deformation of hollow polyelectrolyte microcapsules using an atomic force microscope [37]. In the case of the nanosphere, the photoinduced deformation effect restricted to a very small surface produces a different behavior

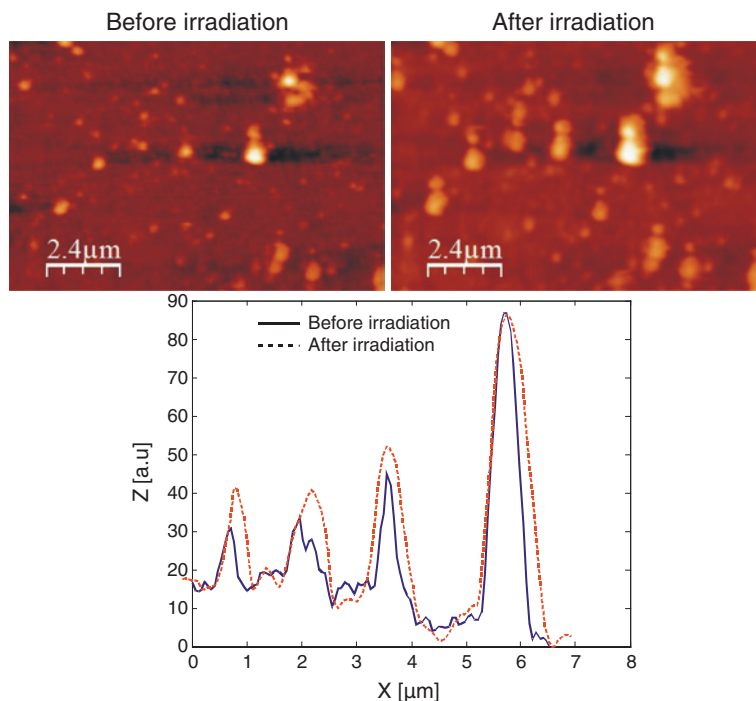


Fig. 7.13 AFM profiles in the X direction of nanospheres before and after irradiation with an incoherent along the substrate plane

than in thin films. A white light incoherent beam can be used for uniform mass motion. The conclusion of this experiment shows that the use of incoherent light is a promising technique in the case of formation or patterning of nano-objects with dimensions in the order of the coherence property of light.

7.4.3 Other Nano-Objects

A simple bottom-up approach has been experimentally demonstrated to form donut-shaped nanostructures at the tailored surface of an azopolymer film by an incoherent unpolarized light illumination. The key difference in this approach is the use of an incoherent light for growing nanostructures rather than for optical erasing and simultaneously directing the final shape of a nanostructure by the initial seed of tiny nanoscale holes. The surface of the film was covered with randomly placed nanoholes with a monodispersed diameter but with different depths. The method chosen is solvent-induced dewetting of thin azopolymer films on glass substrates. Contact of a thin polymer film to its solvent droplet reduces the glass transition

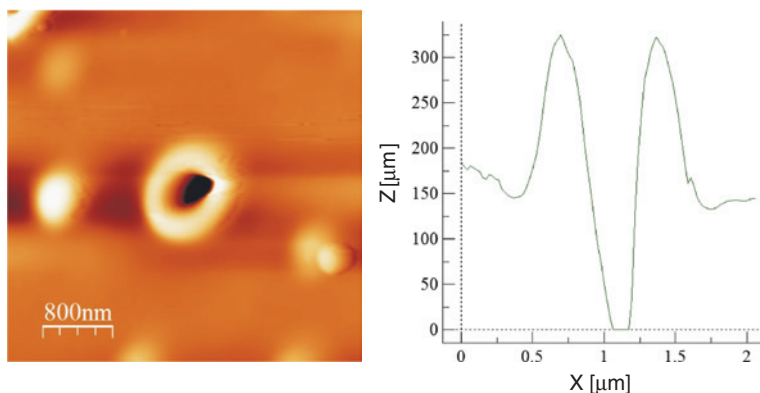


Fig. 7.14 A typical close-up topographical image of azopolymer nanodoughnut obtained by AFM and corresponding height cross section

temperature as the solvent molecules penetrate into the film matrix. The length scale period between the nanohole structures is a function of the film thickness as well as the surface and interfacial tensions of the film and the substrate material.

In the experiment, incoherent white light from xenon halogen lamp was used to initiate photoinduced mass transport in the film. To prove the ability of photoinduced nanostructuring, a detailed AFM image of the film after the illumination was made (Fig. 7.14). Nanodonuts represent a structure which consists of a central hole and a surrounding ring. According to the photoinduced material used in the experiment, the geometry of the nanostructures can be modified by light.

7.5 Conclusion

In conclusion, azopolymer is a photoinduced material giving a large number of possibilities to manage the fabrication and modification of nano-objects. A large number of geometric shapes and topologies of nano-objects can be fabricated. Moreover, this material opens the way to the emerging field of polymer nanostructuring with the ability to generate a variety of different morphologies with structural definition on the nanometric scale. Properties and behaviors of this material used for nanometric structures depend on both the nature of its molecular constituents and their precise spatial self-positioning. We have shown that these unique features are mainly obtained by molecular mass transport due to a *trans-cis* isomerization. Nanostructured materials can lead to the development of new miniature devices. For example, nanotube or tubular nanodevices can be functionalized with organic/inorganic materials to combine fluorescent multi-properties [38]. With the progress in synthesis routes, it is possible to reproduce and easily fabricate and study nanostructured polymer systems, such as thin films, nanowires, nanotubes, and nanoparticles.

References

1. S.F.Y. Li, S.S. Mark, L.J. Kricka, Polymeric nanotubes and nanorods for biomedical applications. *Cur. Nanosci.* **5**, 182–188 (2014)
2. A. Primagi, A. Shevchenko, Azopolymer-based micro—and nanopatterning for photonic applications. *J. Polym. Sci. Part B: Polym. Phys.* **52**(3), 163–182 (2014)
3. H. Zollinger, *Azo and diazo chemistry: aliphatic and aromatic compounds* (Interscience Publishers, New York, 1961)
4. N.K. Viswanathan, D.Y. Kim, S. Bian, J. Williams, W. Liu, L. Li, L. Samuelson, J. Kumar, S.K. Tripathy, Surface relief structures on azo polymer films. *J. Mater. Chem.* **9**, 1941–1955 (1999)
5. X. Wang, J. Yin, X. Wang, Self-structured surface patterns on epoxy-based azo polymer film-induced by laser light irradiation. *Macromolecules* **44**, 6856–6867 (2011)
6. R.J. Moerland, J.E. Koskela, A. Kravchenko, M. Simberg, S. van der Vegte, M. Kaivola, A. Priimagi, R.H.A. Ras, Large-area arrays of three-dimensional plasmonic subwavelength-sized structures from azopolymer surface-relief gratings. *Mater. Horiz.* **1**, 74–80 (2014)
7. G. Ye, C. Yang, X. Wang, Sensing diffraction gratings of antigen-responsive hydrogel for human immunoglobulin-g detection. *Macromol. Rapid Commun.* **31**, 1332–1336 (2010)
8. H. PilHo, Y. Fadong, L. Lian, K. Myunghwan, R. Mosurkal, A.L. Samuelson, J. Kumar, Simple fabrication of zinc oxide nanostructures. *J. Mater. Chem.* **18**, 637–639 (2008)
9. Z. Sekkat, S. Kawata, Laser nanofabrication in photoresists and azopolymers. *Laser Photonics Rev.* **8**(1), 1–26 (2014)
10. R.H. Lambeth, J. Park, H. Liao, D.J. Shir, S. Jeon, J.A. Rogers, J.S. Moore, Proximity field nanopatterning of azopolymer thin films. *Nanotechnology* **21**, 165301 (2010)
11. S. Ahmadi Kanjani, R. Barille, B.S. Dabos-Seignon, J.-M. Nunzi, E. Ortyl, S. Kucharski, Multistate polarization addressing using one single beam in an azopolymer film. *Opt. Lett.* **30**(15), 1986–1988 (2005)
12. S. Ahmadi Kanjani, R. Barille, B.S. Dabos-Seignon, J.-M. Nunzi, E. Ortyl, S. Kucharski, Incoherent light induced self-organisation of molecules. *Opt. Lett.* **30**(23), 3177–3179 (2005)
13. E. Heydari, E. Mohajerani, A. Shams, All optical switching in azo-polymer planar waveguide. *Opt. Comm.* **284**(5), 1208–1212 (2011)
14. Y. Luo, J. Zhou, Q. Yan, W. Su, Z. Li, Q. Zhang, J. Huang, K. Wang, Optical manipulable polymer optical fiber Bragg gratings with azopolymer as core material. *Appl. Phys. Lett.* **91**, 071110 (2007)
15. R. Barille, Y. Morille, D.G. Perez, S. Kucharski, S. Zielinska, E. Ortyl, Simple turbulence measurements with Azopolymer thin films. *Opt. Lett.* **38**(7), 1128–1130 (2013)
16. A. Consortini, Y.Y. Sun, G. Conforti, A mixed method for measuring the inner scale of atmospheric turbulence. *J. Mod. Opt.* **37**(10), 1555–1560 (1990)
17. R. Barille, R. Janik, S. Kucharski, J. Eyer, F. Letournel, Photo-responsive polymer with erasable and reconfigurable micro- and nano-patterns: An in vitro study for neuron guidance. *Colloids Surf. B.* **88**(1), 63–71 (2011)
18. R. Janik, S. Kucharski, A. Sobolewska, R. Barille, Chemical modification of glass surface with a monolayer of nonchromophoric and chromophoric methacrylate terpolymer. *Appl. Surf. Sci.* **257**(3), 861–866 (2010)
19. D.T. Bong, T.D. Clark, J.R. Granja, M.R. Ghadiri, Self-assembling organic nanotubes. *Angew. Chem. Int. Ed.* **40**, 988 (2001)
20. J. Martín, J. Maiz, J. Sacristan, C. Mijangos, Tailored polymer-based nanorods and nanotubes by “template synthesis”: from preparation to applications. *Polymer* **53**, 1149–1166 (2012)
21. M. Steinhart, J.H. Wendorff, A. Greiner, R.B. Wehrspohn, K. Nielsch, J. Schilling, J. Choi, U. Gösele, Polymer nanotubes by wetting of ordered porous templates. *Science* **296**(5575), 1997 (2002)
22. Banu S, Birtwell S, Chen Y, Galitonov G, Morgan H, Zheludev N (2006) High capacity nano-optical diffraction barcode tagging for biological and chemical applications, *NSTI-Nanotech*, 1

23. R. Barillé, P. Tajalli, J.M. Nunzi, S. Zielińska, S. Kucharski, E. Ortyl, surface relief grating on azopolymer nanosurface. *Appl. Phys. Lett.* **95**, 053102 (2009)
24. I. Freund, M. Deutsch, A. Sprecher, Connective tissue polarity. Optical second-harmonic microscopy, crossed-beam summation, and small-angle scattering in rat-tail tendon. *Biophys. J.* **50**, 693–712 (1986)
25. H.M. Liem, P. Etchegoin, K.S. Whitehead, D.C. Bradley, Raman anisotropy measurements: An effective probe of molecular orientation in conjugated polymer thin films. *Adv. Funct. Mater.* **3**(1), 66–72 (2003)
26. M.I. Klima, A.V. Kotov, L.A. Gribov, Analysis of the vibrational spectrum of azobenzene. *J. Struct. Chem.* **13**(6), 987–990 (1973)
27. C.M. Stuart, R.R. Frontiera, R.A. Mathis, Excited-state structure and dynamics of cis- and trans-azobenzene from resonance Raman intensity analysis. *J. Phys. Chem. A* **111**, 12072–12080 (2007)
28. S. Frisk, R.M. Ikeda, D.B. Chase, J.F. Rabolt, Determination of the molecular orientation of Poly(propylene terephthalate) fibers using polarized Raman spectroscopy: a comparison of methods. *Appl. Spect.* **58**(3), 279–286 (2004)
29. M. Janko, P. Davydovskaya, M. Bauer, A. Zink, R.W. Stark, Anisotropic Raman scattering in collagen bundles. *Opt. Lett.* **35**(16), 2765–2767 (2010)
30. R.D. Schaller, R.J. Saykally, Y.R. Shen, F. Lagugné-Labarhet, Poled polymer thin-film gratings studied with far-field optical diffraction and second-harmonic near-field microscopy. *Opt. Lett.* **28**(15), 1296–1298 (2003)
31. F. Eisert, O. Dannenberger, M. Buck, Molecular orientation determined by second-harmonic generation: Self-assembled monolayers. *Phys. Rev. B* **58**(16), 10860–10870 (1998)
32. J. Prasad Rao, K.E. Geckeler, 'Polymer nanoparticles preparation techniques and size-control parameters'. *Prog. Polym. Sci.* **36**, 887–913 (2011)
33. M. Alcoutlabi, G.B. McKenna, Effects of confinement on material behaviour at the nanometer size scale. *J. Phys.: Condens. Matter* **17**(15), R461 (2005)
34. C. Zhang, Y. Guo, R.D. Priestley, Glass transition temperature of polymer nanoparticles under soft and hard confinement. *Macromolecules* **44**(10), 4001–4006 (2011)
35. C. Zhang, Y. Guo, R.D. Priestley, Characteristic length of the glass transition in isochorically confined polymer glasses. *ACS Macro Lett.* **3**, 501–505 (2014)
36. L. Zhang, A. Eisenberg, Multiple morphologies of "crew-cut" aggregates of polystyrene-*b*-poly(acrylic acid) block copolymers. *Science* **268**, 1728 (1995)
37. V.V. Lulevich, I.L. Radtchenko, G.B. Sukhorukov, O.I. Vinogradova, Deformation properties of nonadhesive polyelectrolyte microcapsules studied with the atomic force microscope. *J. Phys. Chem. B* **107**, 2735 (2003)
38. A. Garreau, F. Massuyeau, S. Cordier, Y. Molard, E. Gautron, P. Bertoncini, E. Faulques, J. Wery, B. Humbert, A. Bulou, J.L. Duvail, Color control in coaxial two-luminophore nanowires. *ACS Nano.* **7**(4), 2977–2987 (2013)